BUTTERWORTH HEINEMANN

Numerical simulation of forced wakes around a cylinder

O. Inoue, T. Yamazaki, and T. Bisaka
Institute of Fluid Science, Tohoku University, Japan

Two-dimensional, incompressible Navier–Stokes equations are solved numerically by finite difference method to study effects of periodic forcing on the development of wakes past a circular cylinder. Forcing is applied either by blowing/suction from the surface of the cylinder or by perturbing the uniform velocity of a free stream. Results suggest that merging of vortices shed from the cylinder, and, thus, development of wakes, are effectively controlled by periodic forcing. Forcing frequencies higher than the primary frequency of the Karman vortex street (hereafter referred to as the Karman frequency) are found to be effective to control near-wakes, while those lower than the Karman frequency are found to control far-wakes. It is also found that by controlling near-wakes, drag working on the cylinder can be reduced and becomes minimum at a forcing frequency that depends on the Reynolds number.

Keywords: cylinder wakes; Navier–Stokes simulations; periodic forcing; vortex merging; drug reduction

Introduction

Increasing attention has been paid to the effects of forcing on the roll-up and subsequent merging of vortices in separated shear layers and wakes, because forcing may have a potential to change the flow structures drastically and to provide turbulence control and drag reduction. For example, Matsui and Okude (1982) observed in their experimental study of a wake past a circular cylinder that, when the wake is forced by one half or one third of the Karman frequency, the number of vortices merging in the subsequent secondary vortex street is two or three, depending on the forcing frequency. Leu and Ho (1993) observed that by applying suction at the end of a splitter plate, flow features of a mixing layer or a wake are drastically changed. In their experiments of vibrating circular cylinders, Nakano and Rockwell (1991, 1993) observed that amplitude- or frequency-modulated excitation has a profound effect on the evolution of the vortex street behind the cylinder. For a comprehensive review of forced shear flows and wakes, readers are referred to Ho and Huerre (1984) and Oertel (1990). In this study, the effect of periodic forcing on the development of near- and far-wakes of a circular cylinder is studied numerically. Special emphasis is placed on the effects of forcing frequency on the formation and merging of vortices in the wakes.

Mathematical formulation and numerical procedure

We consider a two-dimensional (2-D), viscous, incompressible flow past a circular cylinder. Two different types of forcing are considered: a periodical blowing/suction from the surface of the cylinder for a near-wake control and a periodic perturbation of the upstream velocity for a far-wake control. In Figure 1, a schematic of flow model for the case of near-wake control is presented. A blowing/suction is applied at the positions of $\pm 80°$ from the leading edge, around which an unforced flow is likely to be separated. On the other hand, for the case of far-wake control, velocity perturbation of the form $u = U_\infty + u_f$ was applied at the inlet boundary. In both cases of near- and far-wake controls, forcing velocities are assumed to be of the following form (Inoue 1992):

$$u_f,\ v_f = A_0 \sin(2\pi f_0 t) + A_1 \sin(2\pi f_1 t + \beta_1) \qquad (1)$$

where t is the time. Flow quantities are nondimensionalized by the uniform velocity U_∞ of a free stream and the cylinder diameter D. The Reynolds numbers were prescribed to be $\mathrm{Re} = 140$ for comparison with the experiment of Matsui and Okude (1982), and 10^4 and 2×10^4.

The Navier–Stokes equations are solved by a finite difference method based on a SMAC algorithm. The O-type grid system with 401×101 grid points was used for the case of near-wake control, while the case of far-wake control the combination of the O-type grid (with 401×201 grid points) around the cylinder and the rectangular grid system (with 1841×161) was used for far-wake region. The boundary conditions for unforced flows were prescribed as follows:

on the cylinder surface:

$$u = 0, \qquad v = 0$$

on the side boundaries:

$$\frac{\partial u}{\partial y} = 0, \qquad \frac{\partial v}{\partial y} = 0, \qquad p = 0$$

on the inlet boundary:

$$u = 1, \qquad v = 0, \qquad \frac{\partial p}{\partial x} = 0$$

Address reprint requests to Prof. Osamu Inoue, Institute of Fluid Science, Tohoku University, 2-1-1 Katahira, Aoba-ku, Sendai 980-77, Japan.

Received 18 January 1995; accepted 11 April 1995

Int. J. Heat and Fluid Flow 16: 327–332, 1995

655 Avenue of the Americas, New York, NY 10010

0142-727X/95/$10.00
SSDI 0142-727X(95)00054-T

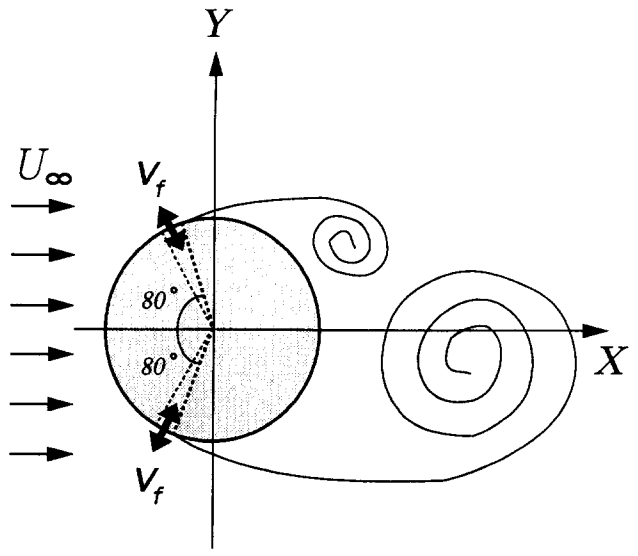

Figure 1 Schematic of flow model for the case of near-wake control

on the exit boundary:

$$\frac{\partial u}{\partial x} = 0, \qquad \frac{\partial v}{\partial x} = 0, \qquad p = 0 \tag{2}$$

Pressure on the cylinder surface was determined by linear extrapolation. In this study, we assumed a test section where flow quantities are measured accurately, and downstream of the test section we added a buffer region where the Karman vortices are forced to die out by increasing grid sizes with the downstream distance. The outflow condition given in Equation 2 was applied at the end of the buffer region. The lengths of the test section and the buffer region were determined so that the existence of the buffer region and the outflow condition do not affect the flow quantities in the test section. The boundary conditions for forced cases were modified from Equation 2, as follows:

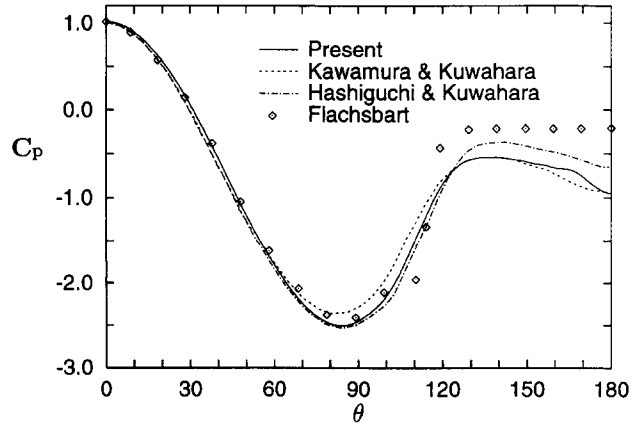

Figure 2 Surface pressure distributions for unforced cylinder wakes, Re = 6.7×10^5; ———, present; - - - - -, Kawamura and Kuwahara (1984); — - —, Hashiguchi and Kuwahara (1992); ◇, Flachsbart (1929)

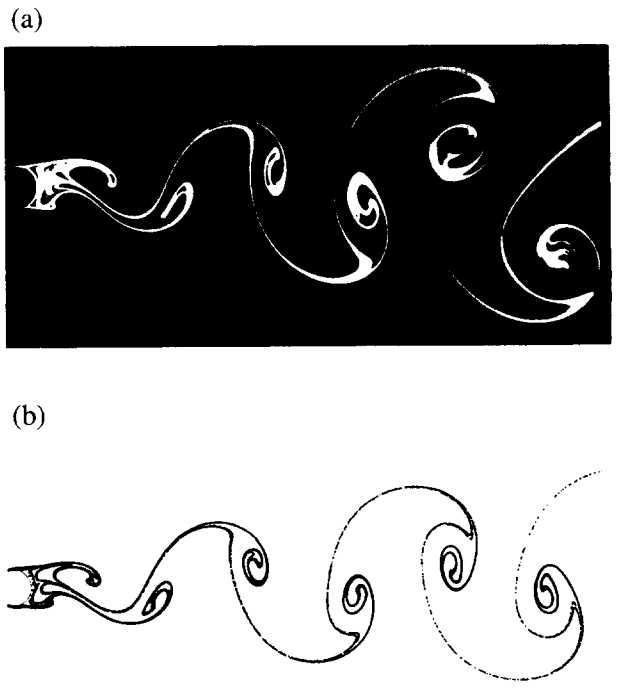

Figure 3 Undisturbed wakes past a circular cylinder, Re = 140; (a) experiment by Taneda; (b) computation

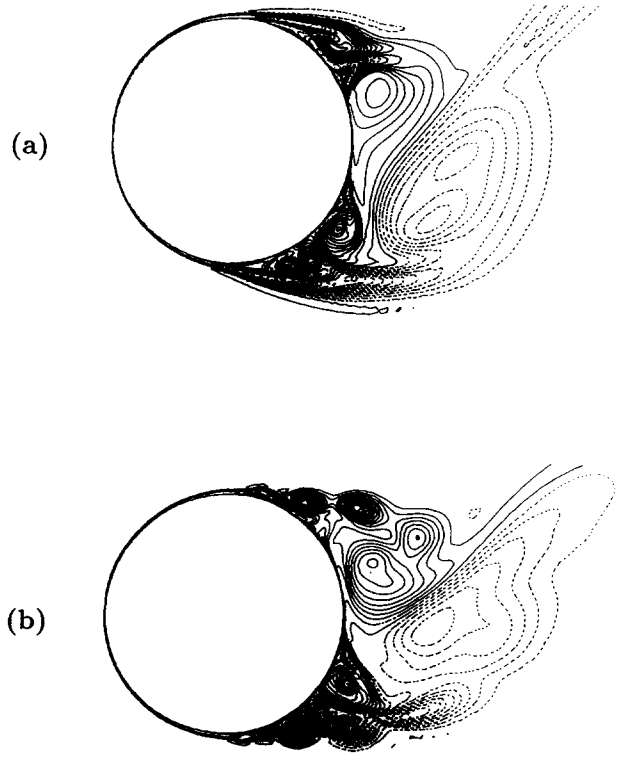

Figure 4 Instantaneous vorticity plots in the near-wake region, Re = 2×10^4; (a) unforced flow; (b) single-frequency forced flow with $A_0 = 0.1$ and $f_0 = 3.0$

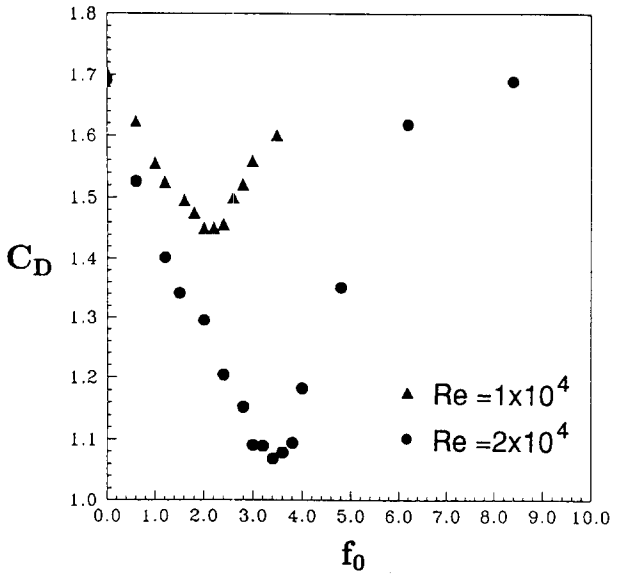

Figure 5 Dependency of drag coefficient on forcing frequency, $A_0 = 0.1$; ▲: $Re = 10^4$; ●: $Re = 2 \times 10^4$

for near-wake control:

$u = 0, \quad v = v_f$ at $\theta = \pm 80°$ on the cylinder surface

for far-wake control:

$u = v_f \cos\theta, \quad v = v_f \sin\theta$ on the inlet boundary

A predictor–corrector scheme of the Crank–Nicolson type was used for time integration. Time step was prescribed to be $\Delta t = 0.002 - 0.005$.

Results and discussion

Control of near-wake

Before proceeding to the forced case, we examined accuracy of our computation by comparing our calculated results of unforced wakes with those of others and also with experiments. Pressure distributions along the cylinder surface for the case of $Re = 6.7 \times 10^5$ are shown in Figure 2. As is readily seen, the present result gives reasonably good agreement with the experiment. Figure 3 is a flow pattern calculated for the case of an unforced wake with the Reynolds number $Re = 140$, together with the corresponding experimental observation by Taneda (Van Dyke 1982). The calculated streaklines were obtained by tracking the movement of marker particles that were shed at every time-step from inside of the boundary layer on the cylinder, sufficiently upstream of a separation point. The velocity of a marker particle was assumed to be the same as the flow velocity at the particle's position at each time. It is seen in Figure 3 that both calculated and experimental streaklines are in excellent qualitative agreements. These results indicate that our computation is reliable, at least qualitatively.

Instantaneous vorticity contours for the cases of unforced and single-frequency forced wakes with $Re = 2 \times 10^4$ are presented in Figure 4. For the case of an unforced flow, the Karman frequency F_K is approximately $F_K = 0.22$. It is seen in Figure 4 that, by applying the periodic forcing with a sufficiently large amplitude, shear layers separated from the cylinder surface roll-up to form discrete vortices regularly. The roll-up frequency of the vortices is the same as the forcing frequency.

Drag coefficient C_D for single-frequency forced cases with a fixed value of $A_0 = 0.1$ is presented *versus* f_0 in Figure 5. In the figure, the filled circle denotes the case of $Re = 2 \times 10^4$, and the filled triangle denotes the case of $Re = 10^4$. As seen from the

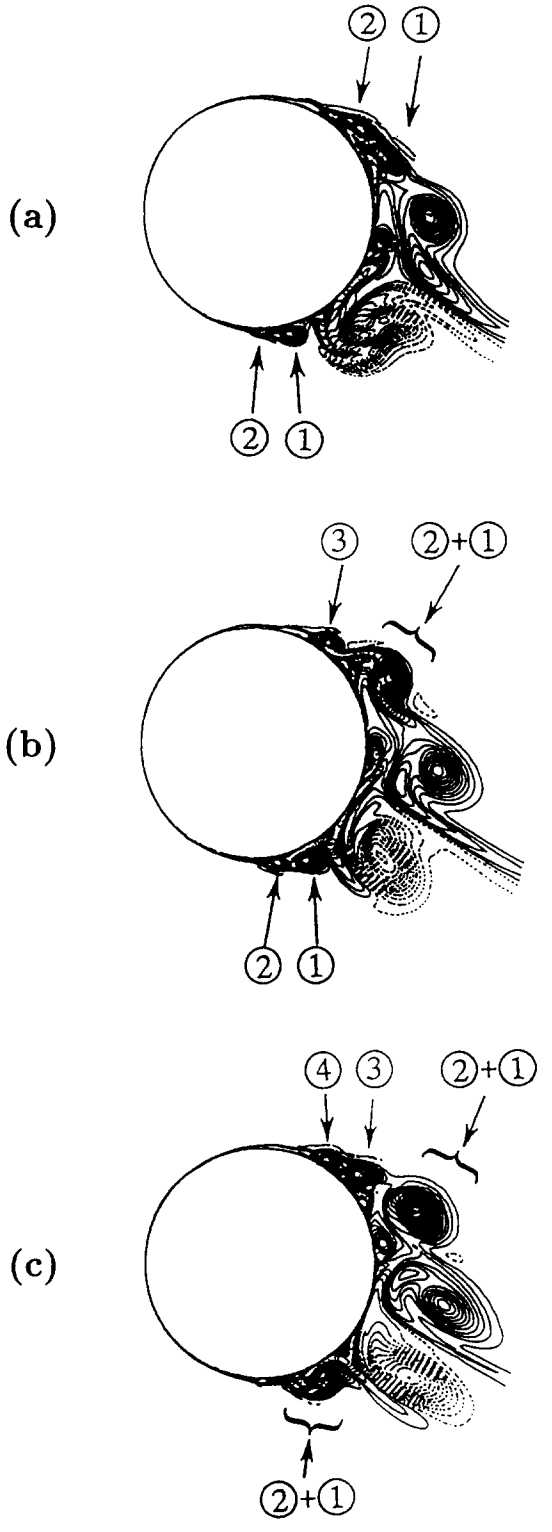

Figure 6 Regular vortex merging in the near-wake region of a double-frequency forced flow, vorticity contours, $Re = 2 \times 10^4$; $A_0 = A_1 = 0.1$, $f_0 = 3.0$, $f_1 = f_0/2$, $\beta_1 = 0$; (a) $t = 383.2$; (b) $t = 383.4$; (c) $t = 383.6$

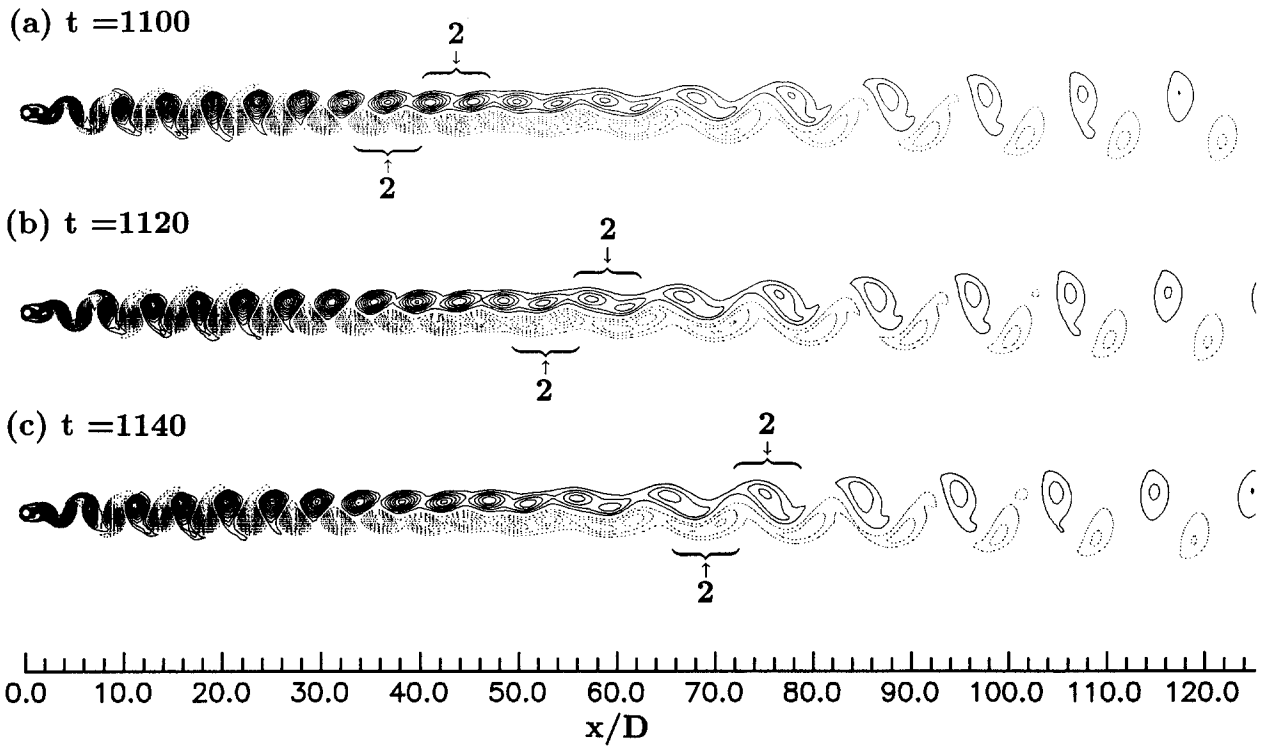

Figure 7 Vorticity contours for the case of $f_0 = F_K/2$, Re = 140, $A_0 = 0.1$

figure, C_D decreases with increasing forcing frequency and becomes minimum at around $f_0 = 3.4$ for the case of $\mathrm{Re} = 2 \times 10^4$ and at around $f_0 = 2.2$ for the case of $\mathrm{Re} = 10^4$. In both cases of Re, the frequency $F_{\min}$ at which C_D becomes minimum is, respectively, much higher than the Karman frequency $F_K (\cong 0.22)$ of the corresponding unforced flows. This result suggests that drag reduction is affected by the vortical motion in the near-wake where the roll-up frequency of the separated shear layer is much higher than the Karman frequency. The minimum value of the drag coefficient is about 85% that of the unforced flow for $\mathrm{Re} = 10^4$ and about 60% for $\mathrm{Re} = 2 \times 10^4$. Beyond $F_{\min}$, C_D recovers with further increasing forcing frequency.

Instantaneous vorticity contours of a double-frequency forced wake with $f_0 = 3.0$, $f_1 = 1.5$ $(= f_0/2)$ and $\beta_1 = 0$ are plotted in Figure 6 for the case of $\mathrm{Re} = 2 \times 10^4$. As seen in the figure, when a primary frequency f_0 is combined with its first subharmonic $f_0/2$, every two vortices that are rolled up at the primary frequency f_0 tend to merge regularly. The regular merging of vortices had been observed in mixing layers (Ho and Huang 1982; Inoue 1992). The drag coefficient C_D in this case was

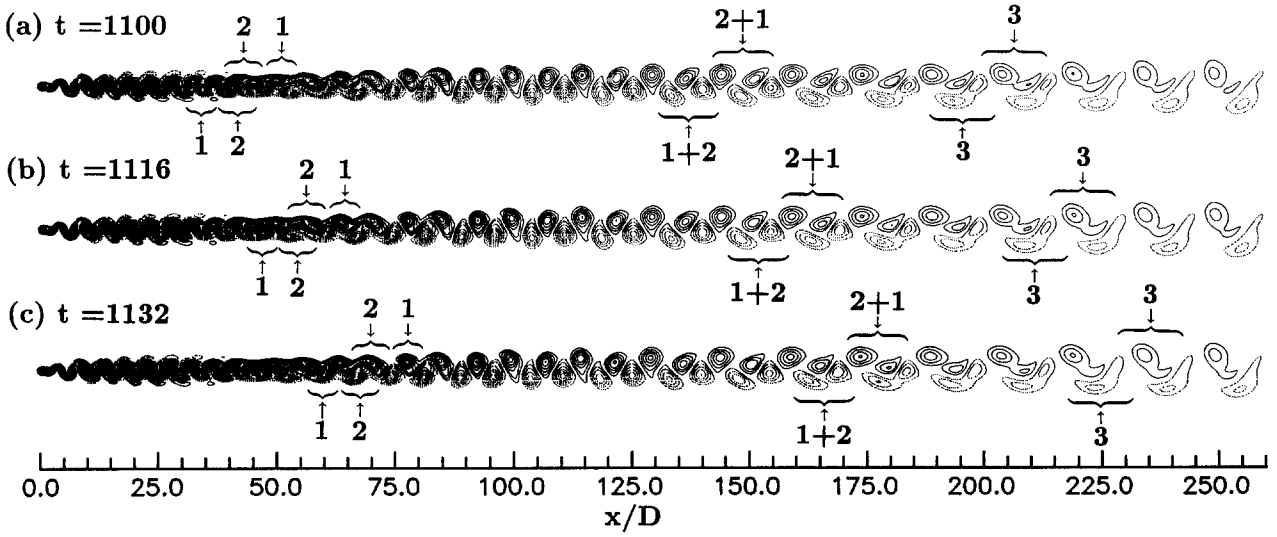

Figure 8 Vorticity contours for the case of $f_0 = F_K/3$, Re = 140, $A_0 = 0.1$

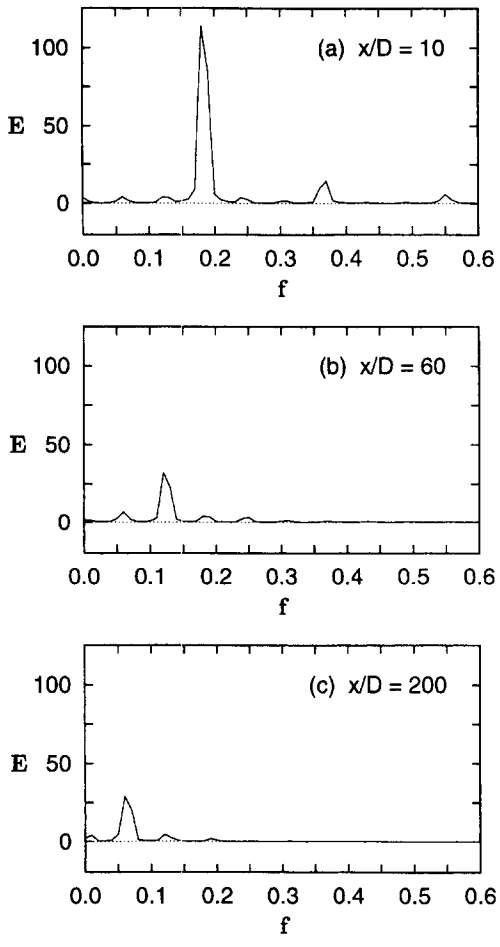

Figure 9 Energy spectra of velocity fluctuations for the case of $f_0 = F_K/3$, Re = 140, $A_0 = 0.1$; (a) $x/D = 10$; (b) $x/D = 60$; (c) $x/D = 200$

1.26, which is higher than the value at $f_0(C_D \approx 1.09)$ and lower than that at $f_1(C_D \approx 1.34)$ both for single-frequency forced cases presented in Figure 5.

Control of far-wake

As mentioned in the Introduction, Matsui and Okude (1982) observed that, when the cylinder wake is forced by subharmonics of the Karman frequency F_K, vortices merge regularly, and the number of merging vortices depends on the subharmonics: that is, every two vortices merge when forced by $F_K/2$, every three vortices merge when forced by $F_K/3$. To compare our calculated results with the experiment of Matsui and Okude, we prescribe the forcing frequency to be F_K/n ($n = 2, 3, \ldots$) and the Reynolds number to be 140. Time development of vorticity fields for the cases of $f_0 = F_K/2$ and $f_0 = F_K/3$ are presented in Figures 7 and 8, respectively. In the figures, upper and lower arrows, respectively, present time development of merging vortices, and numerals denote the number of merging vortices. As readily seen from the figures, every two vortices merge when $f_0 = F_K/2$ (Figure 7) and every three vortices merge when $f_0 = F_K/3$ (Figure 8), in agreement with the experimental observation by Matsui and Okude. Figure 9 shows the energy spectra of velocity fluctuations for the same case as in Figure 8. In the figure, E denotes the spectral amplitude. The streamwise locations where energy spectra were measured are $x/D = 10$, where the primary Karman vortex street is almost established, $x/D = 60$ where merging of two vortices among three is in progress, and $x/D = 200$ where three vortices merging is in progress. As seen from Figure 9a, the energy spectrum has a peak at $f = F_K$ (≈ 0.18) in the primary Karman vortex street. Figure 9b shows that at $x/D = 60$ the energy spectrum has a peak at $f = 2F_K/3$ (≈ 0.12), in agreement with the occurrence of two vortices merging. Similarly, at $x/D = 200$ the spectrum has a peak at $f = F_K/3$ (≈ 0.06), as seen from Figure 9c. In Figure 10, instantaneous vorticity contours are presented for the double-frequency forced case of the Karman frequency combined with its first subharmonic frequency (Figure 10a) and high-harmonic frequency (Figure 10b). As seen in Figure 10a, when $f_0 = F_K$ and $f_1 = F_K/2$, every two vortices

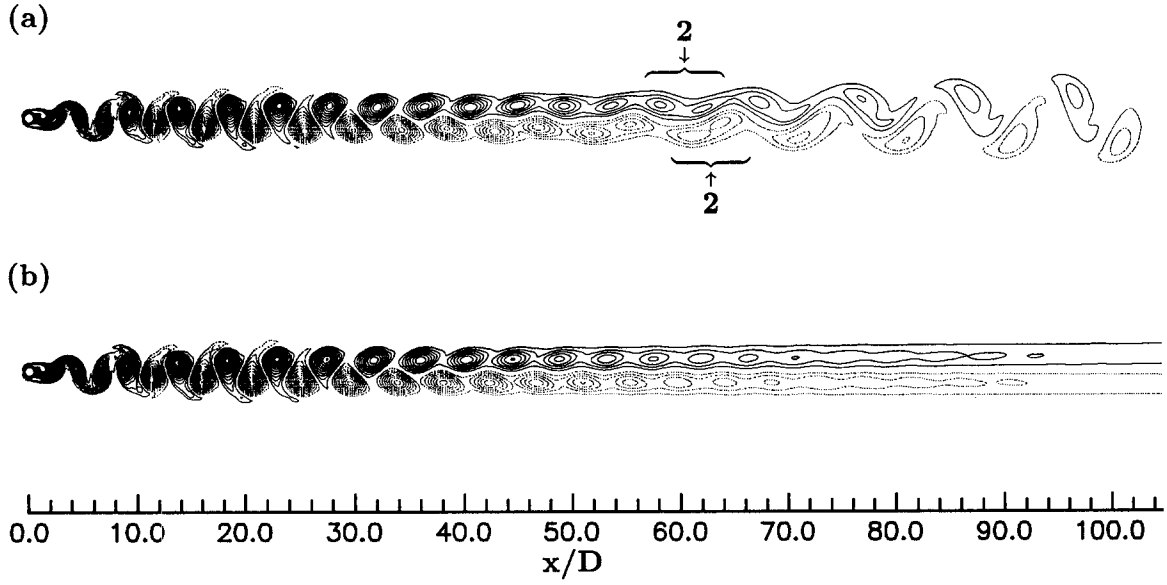

Figure 10 Vorticity contours for the case of double-frequency forcing, Re = 140, $A_0 = A_1 = 0.1$, $\beta_1 = 0$; (a) $f_0 = F_K$, $f_1 = F_K/2$; (b) $f_0 = F_K$, $f_1 = 2F_K$

merge regularly, as in the single-frequency forced case of $f_1 = F_K/2$ (Figure 7). On the other hand, as seen from Figure 10b, when $f_0 = F_K$ and $f_0 = 2F_K$ the Karman vortices did not show any clear evidence of vortex merging, indicating the small influence of the high harmonics on the development of far-wakes.

Conclusion

Effects of periodic forcing on cylinder wakes were investigated by 2-D Navier–Stokes simulations. The results show that the number of merging vortices both in near- and far-wakes can be controlled by periodic forcing. The results for far-wakes agree well with the experimental observation of Matsui and Okude (1982), at least qualitatively. It is found that forcing frequencies higher than the Karman frequency F_K are effective to control near-wakes, while those lower than F_K control far-wakes. It is also found that by controlling near-wakes, drag working on the cylinder can be reduced and becomes minimum at a forcing frequency that depends on the Reynolds number.

References

Flachsbart, O. 1929. Experiments on the flow past a circular at very high Reynolds number (from an article by A. Roshko 1961). *J. Fluid Mech.*, **10**, 350

Hashiguch, M. and Kuwahara, K. 1992. Numerical computation of high Reynolds number flow by using multidirectional upwind finite difference method. *Proc. 6th Symposium on Computational Fluid Dynamics*, 567–570, (in Japanese)

Ho, C. M. and Huerre, P. 1984. Perturbed free shear layers. *Annu. Rev. Fluid Mech.*, **16**, 365–424

Ho, C. M. and Huang, L. S. 1982. Subharmonics and vortex merging in mixing layers. *J. Fluid Mech.*, **119**, 443–473

Inoue, O. 1992. Double-frequency forcing on spatially growing mixing layers. *J. Fluid Mech.*, **234**, 553–581

Kawamura, T. and Kuwahara, K. 1984. Computation of high Reynolds number flow around a circular cylinder with surface roughness. AIAA Paper, No. 84-0340

Leu, T. S. and Ho, C. M. 1993. Control of a 2-D wake by suction at the trailing edge of a splitter plate. Proc. *9th Symposium on Turbulent Shear Flows*, Kyoto, Japan, 20.1.1–20.1.6

Matsui, T. and Okude, M. 1982. Formation of the secondary vortex street in the wake of a circular cylinder. *Proc. IUTAM Symposium on Structures of Compressible Turbulent Shear Flow*, Marseille, France, Springer, Berlin, 156–164

Nakano, M. and Rockwell, D. 1991. Destabilization of the Karman vortex street by frequency-modulated excitation. *Phys. Fluids*, **3**, 723–725

Nakano, M. and Rockwell, D. 1993. The wake from a cylinder subjected to amplitude-modulated excitation. *J. Fluid Mech.*, **247**, 79–110

Oertel, Jr. H. 1990. Wakes behind blunt bodies. *Ann. Rev. Fluid Mech.*, **22**, 539–564

Van Dyke, M. 1982. *An Album of Fluid Motion*. Parabolic Press, 56